Flood Inundation Mapping of Low-, Medium-, and High-Flow Events Using the AutoRoute Model

Michael L. Follum[1], Ahmad A. Tavakoly[1,2], Joseph L. Gutenson[1,3], and Ricardo Vera[4]

[1]Coastal and Hydraulics Laboratory, Engineer Research and Development Center, 3909 Halls Ferry Road, Vicksburg, MS 39180, USA
[2]Earth System Science Interdisciplinary Center, University of Maryland, College Park, MD 20740, USA
[3]National Water Center, National Oceanic and Atmospheric Administration, 205 Hackberry Ln, Tuscaloosa, AL 35401, USA
[4]Cold Regions Research and Engineering Laboratory, Engineer Research and Development Center, 72 Lyme Road, Hanover, NH 03755, USA

Correspondence to: Michael L. Follum (follumm@gmail.com)

Abstract. This article presents improvements and development of a post-processing module for the regional scale flood mapping tool, AutoRoute. The accuracy of this model to simulate low, medium, and high flow rate scenarios is demonstrated at seven test sites within the U.S. AutoRoute is one of the tools used to create high-resolution flood inundation maps at regional- to continental-scales. The model has previously only been tested using extreme flood events. In this article flood inundation results for low-flow events are shown to be accurate (average F value of 63.3%) but tend to be overestimated, especially in flatter terrain. Higher-flow scenarios tend to be more accurately simulated (average F value of 77.5%). Additionally, modifications to the AutoRoute model and post-processing scripts are shown to improve computational efficiency (i.e. simulation time) by over 40% when compared to previous versions. With improved computational efficiency and the ability to accurately simulate both low and high flow scenarios the AutoRoute model may be well suited to provide first-order estimates of flooding within an operational, regional- to continental-scale hydrologic modelling framework.

1 Introduction

Recent advances have demonstrated continental-scale flow forecasting models capable of simulating thousands of stream reaches simultaneously (e.g. National Water Model (NWM) (http://water.noaa.gov/about/nwm); Streamflow Prediction Tool (SPT) (Snow et al., 2016; Wahl 2016)). Although flow simulations at these scales are beneficial, water managers and emergency personnel benefit more from high-resolution flood inundation maps to make operational decisions (such as evacuation, road closures, etc.). Advanced hydraulic models typically operated from the reach-scale to the small-basin-scale have shown some success in simulating flood inundation at the continental scale (Wing et al., 2017), but at a high computational cost. Due to low data requirements, fast initial set-up times, and lower computational burden, lower-complexity hydraulic models have been developed in recent years to simulate flood inundation quickly using continental-scale hydrologic modelling outputs. Although not meant to replace the higher-fidelity hydraulic models, these lower-complexity models can provide a

reasonable first-order approximation of flood inundation over regional to continental extents and help prioritize where deployment of the higher-fidelity hydraulic models are needed (Follum et al., 2019). The National Oceanic and Atmospheric Administration (NOAA) National Water Center (NWC) has adopted the Height Above Nearest Drainage (HAND) model (Liu et al., 2018; Zheng et al., 2016) to use in conjunction with the NWM within the U.S. Due to a need for connecting hydrologic

35 data to mobility models for the military, the U.S. Army Coastal and Hydraulics Laboratory (CHL) developed the AutoRoute flood and mobility model (Follum, 2012; Follum et al., 2017). AutoRoute works in conjunction with the SPT (Follum et al., 2017) to provide hydrologic and trafficability guidance outside the continental United Stated (OCONUS) in data sparse environments.

40 Both HAND and AutoRoute are raster-based models. Using the high resolution NHDPlus database (Horizon Systems Corporation, 2007; McKay et al., 2012) and a ~10m digital elevation model (DEM), Liu et al. (2018) created HAND rasters for the entire U.S. A HAND raster simply shows the relative height of a cell above the nearest NHD stream line (nearest in terms of drainage distance). Flow-depth rating curves are assigned to each stream reach (Zheng et al., 2018). Given a flow rate the stage of the river can be calculated and used with the HAND raster to quickly create continuous flood maps. However,

45 this process relies heavily on pre-computed flow-depth relationships that may be difficult to apply in areas without high-resolution DEM or NHD datasets. Additionally, these pre-computed flow-depth relationships must be updated when more accurate or precise DEM or stream line data are made available.

AutoRoute was initially developed by CHL to automatically develop cross-sections along rivers to assess gap-crossing

50 capabilities of military vehicles during flood events (Follum, 2012; McKinley et al., 2012). Recently, AutoRoute has been applied with large-scale river routing models (such as the RAPID model (David et al., 2011; Tavakoly et al., 2017) within SPT) to simulate high-resolution (<30m spatial resolution) flood inundation maps over large extents: 230,000 km^2 area in the Midwest United States; 109,500 km^2 area in the Mississippi Delta (Follum et al., 2017); Sava River Basin; Puerto Rico (Follum et al., 2018); Navajo Nation (Follum et al., 2019); and Luzon, Philippines (Wahl et al., 2017). Stream networks (polyline

55 format) within the U.S. are defined using the NHDPlus dataset. Outside the U.S. stream networks (polyline format) for approximately 70% of the world have been created using HydroSHEDS and HydroBASINS datasets (Lehner and Grill, 2013) (see Snow et al., 2015 for an example). AutoRoute converts the polyline stream locations to a raster or table format (see Follum et al. (2017) for details). Cross-sections are automatically sampled for each stream cell from a DEM and the normal depth is then calculated for a given flow rate using Manning's equation. The extent and depth of flooding within the cross-

60 section is then mapped to a raster format. Only cells within the raster used for cross-sections will show flood extent or depth. A post-processing step is often utilized where flood extent results in raster format are converted to a polygon format. The main purpose of the post-processing step is to overcome inaccuracies in the flood extents created by AutoRoute. Holes in the floodplain (cells not captured by cross-sections) are filled, the boundaries along the floodplain are smoothed, and outliers in the flood extent (cells that show flooding where no other surrounding cells show flooding) are omitted. Outliers in the flood

65   map are caused by large variations in flow depths along a given stream reach (Afshari et al., 2018; Follum et al. 2017), often
caused by high elevation values due to bridges (Follum et al. 2017) or spikes in the DEM; cross-sections not being sampled
perpendicular to the stream channel; and errors in calculating the slope of the channel (related to errors in the stream network
or DEM). It is expected that these variations in depth and flood extent will be more pronounced in low-flow events where
differences in depth or inundation extent may be more evident in an inundation map. Computationally, the post-processing

70   step takes almost as long as the execution of the AutoRoute model itself (Follum et al., 2017). Additionally, this post-
processing step does not consider the terrain data; the post-processing is used only to make flood inundation maps appear more
continuous.

Afshari et al. (2018) compared HAND, AutoRoute (with post-processing), and HEC-RAS 2D (USACE, 2016) at two locations:

75   Cedar River watershed in Iowa, and the Black Warrior River in Alabama. Three statistical flow conditions were tested at each
site, the 10-, 100-, and 500-yr flow rates. The HAND and AutoRoute models produced similar flood inundation maps when
compared to the more-advanced HEC-RAS 2D model, but both HAND and AutoRoute showed less accuracy in meandering
channels and near confluences. Overall, the AutoRoute model produced slightly higher flood extent accuracy than the HAND
model. However, the AutoRoute model tended to have lower accuracy with lower flow events. This highlights a concern that

80   the AutoRoute model has typically been tested for large flood events (flood events greater than the 50-yr flood were tested in
Follum (2012), Follum et al. (2017; 2018; 2019), and Wahl et al. (2017)) and may not be applicable for less extreme flow
events.

This article presents modifications to the AutoRoute model to better incorporate terrain in the post-processing of flood

85   inundation maps and to test the flood mapping capability of the AutoRoute model for extreme (>50 yr flood event) and non-
extreme flood cases. The modifications are expected to produce continuous and accurate flood extent results for both low and
high flow events. The AutoRoute model is tested at seven locations within the U.S. where flood inundation maps for multiple
flow rate scenarios (ranging from low to high flow events) have been modeled and compared to observed flow events by
NOAA's Advanced Hydrologic Prediction Service (McEnery et al., 2005).

90   **2 Methodology**

2.1 AutoRoute Model

AutoRoute is a grid-based model where elevation, stream locations (stream cells), and land cover are defined using a raster
format. Gridded stream cells were originally defined using a flow accumulation raster (Follum, 2012). With the creation of
river networks in polyline format (e.g. NHD and HydroSHEDS) stream cells are now created by converting polyline data to a

95   raster or table format (table defines the x- and y- coordinates). Each stream cell retains the unique river reach identifier (e.g.
ComID in NHD) to associate attributes of the stream reach to each stream cell. For example, streamflow Q (m^3 s^{-1}) from a

hydrologic model, such as SPT or NWM, is assigned to each stream cell using the river reach identifier. At each stream cell, cross-sections are sampled from an elevation dataset (Figure 1). For high flow events the bathymetry in smaller streams can often be ignored because the flow event is considerably higher than the base flow. For low flow events the bathymetry is

100 likely of more importance because the base flow is a larger portion of the flow being simulated. For each cross-section sampled, AutoRoute adjusts the centerline to the lowest point in the cross-section. The lateral distance that AutoRoute searches for the lowest point is specified by the user, typically defined as 20m. As shown in Figure 1, the cross-section sampled from the DEM often shows the stream/river as a flat surface. AutoRoute automatically finds the top-width of the water surface and then estimates a bathymetric profile. The bathymetric profile is assumed to have an exponential shape, as shown in Figure 1.

105 Using Manning's equation (described below), the depth of the bathymetric profile is set so that a specified base flow will pass through the bathymetric profile. The bathymetric profile is burned into the cross-section profile and the centerline of the stream/river is again adjusted to the lowest point.

Hydraulic area A (m²) and wetted perimeter P (m) are calculated at each cross-section for a given flow depth D (m). Using a

110 volume-fill approach D is incrementally increased until there is less than a 1% difference between Q and the calculated streamflow Q_{calc} (m³ s⁻¹), calculated using Manning's Equation:

$$Q_{calc} = \frac{c_u}{n} A^{5/3} P^{-2/3} S_f^{1/2}, \tag{1}$$

where c_u is the unit constant (1.0 for metric units), n is the Manning's roughness coefficient, and S_f is the hydraulic slope. Normal depth is assumed, and therefore $S_f = S_o$, where S_o is the slope of the channel. AutoRoute calculates S_o by analyzing

115 the elevations and lateral distances upstream and downstream of the stream cell being analyzed (more explanation found in Follum et al. (2017)). n is estimated as (Horton, 1933; Einstein, 1934):

$$n = \left[\sum_{i=1}^{N} \frac{P_i n_i^{1.5}}{P} \right]^{2/3}, \tag{2}$$

where P_i and n_i are wetted perimeter and Manning roughness coefficient of the ith segment within the cross-section, and N is the total number of segments within the cross-section that are flooded. n_i values are associated with land cover types, as

120 described in Follum et al. (2017).

An initial cross-section is sampled perpendicular to the stream direction, as defined by positions of upstream and downstream stream cells. However, stream cross-sections may not always adequately capture the floodplain geometry, therefore multiple cross-sections are sampled for each stream cell by incrementally pivoting the cross-section relative to the stream direction. As

125 shown in Follum et al. (2017), these multiple cross-sections have the effect of filling in the floodplain but can also create errant cross-sections and therefore errors in the floodplain mapping. The cross-section for each stream cell (subscript sc) that produces the shortest top width TW_{sc} (m) is expected to be the most representative cross-section for that stream cell. The TW_{sc} and the flow depth D_{sc} (m) of the representative cross-section are recorded for each stream cell.

130 AutoRoute originally created flood inundation and flood depth rasters by mapping all of the cross-section depths and extents onto a raster. An iterative combination of the Boundary Clean and Aggregate Polygons functions within ArcGIS (ESRI, 2011) was then used to fill-in holes, omit outlier flood cells, and smooth boundaries along the flood polygon. None of the previous post-processing considered topography in the creation of the flood polygon.

2.2 Development of AutoRoute post-processing script (ARPP)

135 The AutoRoute post-processing script (ARPP) has been developed to better account for topography when creating the flood inundation map. The water surface elevation of each stream cell WSE_{sc} (m) is calculated:

$$WSE_{sc} = E_c + D_{sc}, \tag{3}$$

where E_c (m) is the elevation of the cell. The water surface elevation for each cell in the model domain (WSE_c, m) is interpolated from the WSE_{sc} values using inverse-distance-weighting:

140 $$WSE_c = \frac{\sum WSE_{sc} w}{\sum w}, \tag{4}$$

where w is the weight, calculated as:

$$\begin{cases} w = d_{c \to sc}^{-2} & if \quad d_{c \to sc} \le \alpha \, TW_{sc} \\ \quad w = 0 & if \quad d_{c \to sc} > \alpha \, TW_{sc} \end{cases} \tag{5}$$

where $d_{c \to sc}$ (m) is the distance between the model domain cell and the stream cell, and α is a user-defined parameter. Higher values of α increase the influence that each stream cell has on flooding the surrounding cells. The flood depth for each cell in

145 the domain D_c (m) is then calculated as:

$$D_c = WSE_c - E_c, \tag{6}$$

where D_c values less than zero are set to zero and cells with D_c values greater than zero are considered flooded. All flooded cells are then converted to a polygon format.

150 Figure 2 (top) demonstrates the flooding (D_c values) of the surrounding terrain from a single stream cell. When the depths from all stream cells are included by use of Eqs. 4 and 5 the flooding of the surrounding cells provides a continuous flood map with holes only in the high-elevation areas (bottom frame of Figure 2). Additionally, stream cells that have WSE_{sc} values higher/lower than surrounding stream cells (i.e. outliers) have minimal impact on flooding the surrounding cells. The minimal impact of outliers is due to the influence of water surface elevations from multiple stream cells on each WSE_c value. Use of

155 ARPP to post-process AutoRoute flood depth results is expected to produce more continuous flood maps, account for topography, and reduce the impact of errant D_{sc} values on the flood inundation results, all of which are expected to be important in simulating both low- and high-flow events.

2.3 Study Locations

For several communities throughout the United States the USGS has created flood inundation maps for multiple water surface
elevations (stages) of the river. These maps are intended to be used in conjunction with National Weather Service (NWS)
forecasted peak-stage data to show predicted areas of flooding. The modelled stage heights vary between the sites, but are
intended to capture the river stage at multiple (often around 20) stages between normal conditions (low flow) and the highest
rated stage at the streamgage (high flow). The hydraulic model used to create the flood inundation maps varies between the
sites, but each model is validated against observed flood events. For this study seven locations where the U.S. Geological
Survey (USGS) has completed flood inundation studies were chosen. Each site varies in complexity as well as geographical
location (multiple river basins throughout the U.S.).

For each site used in this study Table 1 lists the location, identification (ID), river(s), USGS streamgage number, length of
river segments within the study, and reference. All studies utilized LiDAR elevation datasets ranging between 0.9 and 3 m
horizontal spatial resolution. Each study also used the HEC-RAS hydraulic model (USACE, 2010; 2016). Each study
calibrated and validated the hydraulic models to observed flood data.

Table 2 lists the base flow and the low, medium, and high flow rates used in the study. The low, medium, and high flow rates
were chosen based on the minimum, median, and maximum modelled flow rates in each of the USGS studies (a flow rate was
assigned to each stage height in each of the studies). The USGS does not provide base flow estimates for the sites in this study,
so the base flow was estimated as the average annual flow rate for each gage listed in Table 1. The annual flow rates were
obtained from USGS WaterWatch (https://waterwatch.usgs.gov/?id=ww_current; visited 01 Feb 2019). USGS streamgage
02126375 along the Pee Dee River does not record flow rates, so the flow data from the USGS streamgage 0212378405
approximately 12-km upstream along the Pee Dee River was used to estimate baseflow. Brown Creek and Rocky River are
also included in the NC study (Smith and Wagner, 2016), but are omitted from this study because flow rates were unavailable.
The USGS streamgage 02473000 along the Leaf River is used in the MS study and is less than 1 km downstream of the
confluence of the Leaf and Bouie Rivers. Above the confluence of the rivers the Leaf and Bouie Rivers are assumed to carry
approximately 70% and 30%, respectively, of the flow rates measured at the USGS streamgage 02473000 (Storm, 2014).

3 Model Application

AutoRoute models were developed for each of the seven test locations. Each model was developed using elevation data from
the 1/3-arc-second (~9 m) National Elevation Dataset (Gesch et al., 2002), and land cover classifications were obtained from
the 2011 National Land Cover Database (Homer et al., 2015). The stream networks for each study site were defined using the
NHDPlus dataset. The AutoRoute model has few calibration parameters. Following Follum et al. (2017), n_i values were set
to the lower bound as described in Moore (2011), Chow (1959), and Calenda et al. (2005). The number of cross-sections

190   sampled at each stream cell was set to 9 following Follum et al. (2017). The influence that each stream cell has on flooding the surrounding cells is controlled by the user-defined α parameter. When tested, setting α to 1.5 provided good coverage of the river floodplain while remaining computationally efficient.

For each simulation, the qualitative performance of the AutoRoute models compared to the USGS data are measured using the

195   F-statistic (F, percentage) (Bates and De Roo, 2000; Tayefi et al., 2007) and error bias (E) (Wing et al. 2017):

$$F = 100 \left(\frac{A_{Acc}}{A_{Obs} + A_{Sim} - A_{Acc}} \right), \tag{7}$$

$$E = \frac{A_{Over}}{A_{Under}}, \tag{8}$$

where A_{Obs} is the area of flooding from the USGS flood maps, A_{Sim} is the area of flooding from the AutoRoute simulation, A_{Acc} is the area where both AutoRoute and the USGS show flooding, A_{Over} is the area where only the AutoRoute model shows

200   flooding, and A_{Under} is the area where only the USGS flood maps shows flooding. F ranges between 0 and 100% with a value of 100% indicating perfect fit between the AutoRoute and USGS flood inundation maps. Previous applications of AutoRoute within the U.S. have had F values between 58.4 and 92.5% (Follum et al., 2017), with the IN test site having an F value of 77% when compared to observed flood maps from the June 2008 flood. E ranges between 0 and ∞ with E values less than 1 indicating a bias towards underestimation, E values greater than 1 indicating a bias towards overestimation, and an E value

205   of 1 indicating no bias.

4 Results and Discussion

4.1 Flood Inundation Mapping

For each study site the low, medium, and high flow scenarios were simulated using AutoRoute with the results being post-processed using the ARPP. Figures 3-9 show a comparison between the flood inundation maps generated by AutoRoute and

210   the USGS flood maps for the area. In the figures the areas shaded green (Accurate) indicate areas where AutoRoute and the USGS flood maps agree. Areas shaded red (Over) indicate where only AutoRoute simulates the area as flooded and areas shaded blue (Under) indicate where only the USGS shows the area as flooded. Table 3 shows the quantitative performance flood inundation maps simulated using AutoRoute compared to the USGS flood inundation maps.

215   The flood maps generated using low flows are satisfactory (average F value of 63.3%), but tend to overestimate flooding (all E values are greater than 1 except for the CO test site). Although IN has the highest E value, the high F value and Figure 3 show the flood map during the low flow event is accurately simulated and the E value is inflated due to the minimal underestimation of flooding. Visually, NC (Figure 6) and MS (Figure 7) have the greatest amount of overestimation during the low flow event, resulting in the lowest F values of all the simulations. NC shows overestimation in low-lying areas adjacent

220   to the river where the ARPP allows for flooding in areas even if they are not hydraulically connected to the streamlines,

resulting in the lowest overall F value of 39.3%. MS also shows gross overestimation of flooding during the low-flow event. MS has minimal topography, a characteristic that has shown AutoRoute to produce less accurate results (Follum et al., 2017). AutoRoute simulations are essentially one-dimensional (1D), better representation of hydrodynamics in areas with minimal topography occurs with multi-dimensional modelling. Additionally, MS has the highest ratio of low flow to base flow (the low

225 flow used in this study is over 15 times the flow rate of the base flow) which may have led to errors in bathymetry estimation if the elevation dataset was derived during a higher flow event. The coarse resolution used in this study compared to the USGS study may also contribute to inaccuracies (e.g. overestimation) that may be more pronounced in flatter terrain such as MS. While most streams considered in this analysis lie in rural land use environments, such as forested or agricultural areas, MS occurs in a primarily urban to sub-urban environment where small-scale changes in the topography are smoothed or negated

230 in the relatively coarse 10m DEM. Many of these missed topographic features are likely flood control structures, such as levees. The combination of minimal topography, DEM inaccuracies, and land use complexities likely led to the overestimation found in the MS study.

With a few exceptions (e.g. SC (Figure 5)), the flood maps generated for the med- and high-flow events are more accurate

235 than the flood maps generated for the low-flow events. The average F value for med-flow event is 70.0% and average F value for high-flow event is 77.5%. The maximum F value of 92.6% occurs at NC during the med flow (NC had the lowest overall F value during the low-flow event). The sudden increase in F value between the flood maps generated using low-flow and med-flow at NC is due to the low-lying terrain near the river being simulated as flooded by both AutoRoute and the USGS during the med-flow event, thus reducing the overestimation and increasing the accuracy. Although flood maps for the med-

240 and high-flow events tend to have higher F values, they also tend to have a bias to underestimate the flooded area (E values less than 1). The majority of underestimation at the IN test site (Figure 3) occurs where a tributary (Meadowbrook Creek) that is not accounted for in the AutoRoute simulation flows into the White River to the south and west of the town of Spencer.

The two test locations along the Deerfield River in Massachusetts (MC in Figure 8 and MW in Figure 9) show consistent

245 accuracy between the low-, med-, and high-flow rates. This region of Massachusetts has well-defined rivers and medium to high topographic relief. These features allow AutoRoute to better capture the riverbanks and floodplain, resulting in consistent accuracy (F values close to 100) and minimal bias (E values close to 1).

Some inaccuracies in flood inundation results may also be due to the use of constant n_i values that are set solely based on land

250 cover maps. Not only are roughness coefficients likely different even under the same land cover types, but the values of n_i also vary with the depth of water (Ree and Palmer, 1949; Temple et al., 1987). In this study the low estimate of n_i values were used based on Follum et al. (2017). However, that study did not include bathymetry estimation within the cross-sections and therefore a reexamination of the proper of n_i values to use within AutoRoute may be warranted. Another source of error may

be the simple bathymetry estimation for each cross-section. A more detailed bathymetry would affect the low-flow scenario
255 the most but would likely improve the accuracy of flood inundation for all flow scenarios.

4.2 Simulation Time

On average, each flow event for each test case took approximately 12 seconds to read all data (elevation, land cover, stream location, and flow rates) into memory, simulate flood depth results using AutoRoute, post-process the flood depth results into raster flood maps using ARPP, and convert the raster flood maps into flood inundation polygons. However, these model
260 simulations were for relatively small areas whereas the main reason to utilize a simplified hydraulics model such as AutoRoute is for computational efficiency when simulating flood inundation along thousands of river reaches at the regional to continental scales. Therefore, to compare computation times to the original AutoRoute methods described in Follum et al. (2017) the same domains in the Midwest (230,000 km^2 area) and Mississippi Delta (109,500 km^2 area) were simulated again using the methods described in this paper. Similar to Follum et al. (2017) the domains were discretized into thirty-nine 1° by 1° tiles
265 (as defined by how USGS NED data is disseminated). Flow rates from Tavakoly et al. (2017) were once again used to define the peak flow in each river reach in the domain.

The AutoRoute simulations in Follum et al. (2017) required approximately 20-minutes to simulate a 1° by 1° tile, compared to 17.5-minutes using the current version of AutoRoute. The current version of AutoRoute is more computationally efficient
270 through the use of the Geospatial Data Abstraction Library (GDAL/OGR Contributors, 2019) for reading and writing data. The post-processing procedure described in Follum et al. (2017) required approximately 15-minutes for each 1° by 1° tile. Post-processing using ARPP to convert flood depth data to a flood depth raster and flood polygon takes approximately 3 minutes. Overall, the current version of AutoRoute and the use of ARPP is over 40% more computationally efficient in simulating flood inundation maps.

275

The increased computational efficiency of AutoRoute and ARPP along with removing the requirement for ArcGIS software in post-processing may allow for the AutoRoute model to more effectively be implemented at the regional to continental scale. A further improvement may be to create a database of AutoRoute simulations for varying flow rates. When forecast flowrates become available the database could be used instead of an AutoRoute simulation to determine the depth within each stream
280 cell. ARPP could then be used to generate the flood maps. Additionally, a production system could determine if streams within each modelling domain cross a specified bankfull streamflow threshold and AutoRoute simulations would only occur if the streamflows for a given hydrometeorlogical forecast exceeded these bankfull thresholds. Either process may further improve the computational efficiency in creating production flood inundation maps.

5 Conclusions

285   The AutoRoute model is a simplified hydraulics model designed to quickly provide high-resolution flood inundation results at the regional to continental scale. The main purpose of this paper was to test the computational efficiency and accuracy of flood inundation maps generated by the AutoRoute model with special consideration given to less-extreme flow events (i.e. low and medium flood events). Seven test cases were chosen to compare flood inundantion maps using low-, medium-, and high-flow rates. The seven locations correspond to existing USGS flood inundation studies and represent different regions

290   within the U.S. The primary conclusions of the paper are as follows:

1.) Recent updates to the input and output methods within AutoRoute model as well as the post-processing procedure allow for the creation of flood inundation polygons in 20.5 minutes for a 1° by 1° area, as compared to 35-minutes in previous studies. Increased computational efficiency may allow for the AutoRoute model to more effectively be implemented in a production environment at the regional to continental scale.

295   2.) Although the flood inundation results for low-flow events are accurate (average F value of 63.3%), the simulated flooding tends to be overestimated. Higher-flow scenarios tend to be more accurately simulated (F value for med-flow event is 70.0% and average F value for high-flow event is 77.5%). Simplifications in estimating roughness coefficients, cross-section profiles (including bathymetry estimation), and the hydraulic simulation allow for AutoRoute to be computationally efficient but also may lead to errors in flood map simulation.

300   3.) As has been found in other studies, AutoRoute performs best in areas with mid-to-high topographic relief where 1D flood models often perform well. Areas of minimal relief are more susceptible to back-water effects. AutoRoute physics do not account for such physical complexities and model results tend to be less accurate. As such, flood inundation results from AutoRoute should be viewed as a first-order approximation with the use of more detailed hydraulic models providing more actionable flood data.

305   The scope of this research was limited to small and medium inland rivers within the U.S. Several areas of future research were highlighted, including the need to better estimate roughness coefficients based on land cover and with changes in flow depth. Improved bathymetry estimation where no bathymetry data exists could also improve AutoRoute as well as other hydraulic models. Flood inundation models capable of quickly providing high-resolution flood maps have seen great improvement over the past decade as regional- to continental-scale flow simulation models are becoming operationalized by the U.S. Army,

310   NOAA, and others. While the flow and flood inundation models continue to improve, the connection between the flood maps generated and the impacts to the population/environment need to become more fully-developed.

315

Acknowledgements

This project was supported by the Deputy Assistant Secretary of the Army for Research and Technology through the Engineer Research and Development Center's Military Engineering applied research work package title Austere Entry; the Geospatial
320 Intelligence Directorate of the Marine Corps Intelligence Activity; and ERDC's collaborative research project supporting the NOAA National Water Center.

References

325 Afshari, S., Tavakoly, A. A., Rajib, M. A., Zheng, X., Follum, M. L., Omranian, E. and Fekete, B. M.: Comparison of new generation low-complexity flood inundation mapping tools with a hydrodynamic model, J. Hydrol., 556, 539–556, doi:10.1016/j.jhydrol.2017.11.036, 2018.

Bates, P. D. and De Roo, A. P. J.: A simple raster-based model for flood inundation simulation, J. Hydrol., 236(1–2), 54–77, doi:10.1016/S0022-1694(00)00278-X, 2000.

330 Benedict, S. T., Caldwell, A. W. and Clark, J. M.: Flood-inundation maps for the Saluda River from Old Easley Bridge Road to Saluda Lake Dam near Greenville, South Carolina., U.S. Geological Survey Scientific Investigations Map 3244, 2013.

Calenda, G., Mancini, C. P. and Volpi, E.: Distribution of the extreme peak floods of the Tiber River from the XV century, Adv. Water Resour., 28(6), 615–625, doi:10.1016/j.advwatres.2004.09.010, 2005.

335 Chow, V. T.: Open Channel Hydraulics, McGraw-Hill Book Company Inc, New York City, New York, 1959.

David, C. H., Maidment, D. R., Niu, G.-Y., Yang, Z.-L., Habets, F. and Eijkhout, V.: River Network Routing on the NHDPlus Dataset, J. Hydrometeorol., 12(5), 913–934, doi:10.1175/2011JHM1345.1, 2011.

Einstein, H. A.: The Hydraulic Cross Section Radius, Schweizerische Bauzeitung, 103(8), 89–91, 1934.

ESRI: ArcGIS Desktop: Release 10, Environmental Systems Research Institute, Redlands, CA, 2011.

340 Follum, M. L.: AutoRoute Rapid Flood Inundation Model, Coastal and Hydraulics Engineering Technical Note ERDC/CHL CHETN-IV-88. U.S. Army Engineer Research and Development Center, Coastal and Hydraulics Laboratory, Vicksburg, Mississippi 2012.

Follum, M. L., Gutenson, J. L., Wahl, M. D., Hunter, C. J. and Maldonado Linas, J. E.: Rapid Flood Inundation Modeling, Mil. Eng., 110(715), 37–38, 2018.

345 Follum, M. L., Paredez, J. M., Yeates, E. M. and Vera, R.: Utilizing Simple Large-Scale Flood Models to Prioritize Deployment of HEC-RAS 2D Models: Case Study of Navajo Nation Flood Inundation Maps, Flood Risk Management Newsletter , 12(2), 4–7, 2019.

Follum, M. L., Tavakoly, A. A., Niemann, J. D. and Snow, A. D.: AutoRAPID: A Model for Prompt Streamflow Estimation and Flood Inundation Mapping over Regional to Continental Extents, J. Am. Water Resour. Assoc., 53(2), 280–299, doi:10.1111/1752-1688.12476, 2017.

GDAL/OGR Contributors: GDAL/OGR Geospatial Data Abstraction Software Library, Available from: https://gdal.org, 2019.

Gesch, D. B., Oimoen, M., Greenlee, S., Nelson, C., Steuck, M., and Tyler, D: The National Elevation Dataset, Photogrammetric Engineering and Remote Sensing, 68(1):5-32, DOI: 10.1007/978-94-007-6769-0_1, 2002.

Homer, C., Dewitz, J., Yang, L., Jin, S., Danielson, P., Xian, G., Coulston, J., Herold, N., Wickham, J. and Megown, K.: Completion of the 2011 National Land Cover Database for the Conterminous United States – Representing a Decade of Land Cover Change Information, Photogramm. Eng. Remote Sensing, 81(5), 345–354, doi:10.14358/PERS.81.5.345, 2015.

Horizon Systems Corporation: National Hydrography Dataset Plus: Documentation, Available from: http://www.horizon-systems.com/NHDPlus/NHDPlusV1_home.php, 2007.

Horton, R. E.: Separate Roughness Coefficients for Channel Bottom and Sides, Eng. News Rec., 111(22), 652–653, 1933.

Kohn, M. S. and Patton, T. T.: Flood-inundation maps for the South Platte River at Fort Morgan, Colorado, U.S. Geological Survey Scientific Investigations Report 2018–5114, Available from: https://doi.org/10.3133/sir20185114, 2018.

Lehner, B. and Grill, G.: Global river hydrography and network routing: Baseline data and new approaches to study the world's large river systems, Hydrol. Process., 27(15), 2171–2186, doi:10.1002/hyp.9740, 2013.

Liu, Y. Y., Maidment, D. R., Tarboton, D. G., Zheng, X. and Wang, S.: A CyberGIS Integration and Computation Framework for High-Resolution Continental-Scale Flood Inundation Mapping, J. Am. Water Resour. Assoc., 54(4), 770–784, doi:10.1111/1752-1688.12660, 2018.

Lombard, P. J. and Bent, G. C.: Flood-inundation maps for the Deerfield River, Franklin County, Massachusetts, from the confluence with the Cold River tributary to the Connecticut River, U.S. Geological Survey Scientific Investigations Report 2015–5104, Available from: http://dx.doi.org/10.3133/sir20155104, 2015.

McEnery, J., Ingram, J., Duan, Q., Adams, T. and Anderson, L.: NOAA's Advanced Hydrologic Prediction Service, Bull. Am. Meteorol. Soc., 86(3), 375–386, doi:10.1175/BAMS-86-3-375, 2005.

McKay, L., Bondelid, T., Rea, A., Johnston, C., Moore, R. and Deward, T.: NHDPlus Version 2: User Guide., 2012.

McKinley, G. B., Mason, G. L., Follum, M. L., Jourdan, M. R., LaHatte, C. W. and Ellis, J.: A Route Corridor Flood Vulnerability System, Geotechnical and Structures Laboratory Technical Report ERDC/GSL TR-12-29. U.S. Army Engineer Research and Development Center, Geotechnical and Structures Laboratory, Vicksburg, Mississippi, 2012.

Moore, M. R.: Development of a High-Resolution 1D/2D Coupled Flood Simulation of Charles City, Iowa, M.S. Thesis, University of Iowa., 2011.

Nystrom, E. A.: Flood-inundation maps for the White River at Spencer, Indiana, U.S. Geological Survey Scientific Investigations Map 3251, Available from: http://pubs.usgs/gov/sim/3251/, 2013.

Ree, W. and Palmer, V.: Flow of water in channels protected by vegetative linings, U.S. Dept. of Agriculture, No. 967, 1949.

Smith, D. G. and Wagner, C. R.: Hydraulic model and flood-inundation maps developed for the Pee Dee National Wildlife Refuge, North Carolina, U.S. Geological Survey Scientific Investigations Report 2015–5137, Available from: http://dx.doi.org/10.3133/sir20155137, 2016.

385 Snow, A. D.: A New Global Forecasting Model to Produce High-Resolution Stream Forecasts, MS Thesis, Brigham Young University - Provo., 2015.

Snow, A. D., Christensen, S. D., Swain, N. R., Nelson, E. J., Ames, D. P., Jones, N. L., Ding, D., Noman, N. S., David, C. H., Pappenberger, F. and Zsoter, E.: A High-Resolution National-Scale Hydrologic Forecast System from a Global Ensemble Land Surface Model, J. Am. Water Resour. Assoc., 52(4), 950–964, doi:10.1111/1752-1688.12434, 2016.

390 Storm, J. B.: An expanded model—Flood-inundation maps for the Leaf River at Hattiesburg, Mississippi, U.S. Geological Survey Scientific Investigations Map 3300, Available from: http://dx.doi.org/10.3133/sim3228, 2014.

Tavakoly, A. A., Snow, A. D., David, C. H., Follum, M. L., Maidment, D. R. and Yang, Z. L.: Continental-Scale River Flow Modeling of the Mississippi River Basin Using High-Resolution NHDPlus Dataset, J. Am. Water Resour. Assoc., 53(2), 258–279, doi:10.1111/1752-1688.12456, 2017.

395 Tayefi, V., Lane, S. N., Hardy, R. J. and Yu, D.: A comparison of one- and two-dimensional approaches to modelling flood inundation over complex upland floodplains, Hydrol. Process., 21, 3190–3202, doi:10.1002/hyp.6523, 2007.

Temple, D. M., Robinson, K. M., Ahring, R. M. and Davis, A. G.: Stability Design of Grass- lined Open Channels, Agric. Handb., 667, 1987.

U.S. Army Corps of Engineers: HEC-RAS River Analysis System, hydraulic reference manual, 2010.

400 U.S. Army Corps of Engineers: HEC–RAS River Analysis System, hydraulic reference manual, 2016.

Wahl, M. D., Follum, M. L., Snow, A. D. and Tavakoly, A. A.: Developing Hydrologic Awareness, Mil. Eng., 108(700), 2016.

Wing, O. E. J., Bates, P. D., Sampson, C. C., Smith, A. M., Johnson, K. A. and Erickson, T. A.: Validation of a 30 m resolution flood hazard model of the conterminous United States, Water Resour. Res., 53(9), 7968–7986, doi:10.1002/2017WR020917, 2017.

405 Zheng, X., Maidment, D. R., Tarboton, D. G., Liu, Y. Y. and Passalacqua, P.: GeoFlood: Large-Scale Flood Inundation Mapping Based on High-Resolution Terrain Analysis, Water Resour. Res., 54(12), 10,013-10,033, doi:10.1029/2018WR023457, 2018.

Zheng, X., Maidment, D., Liu, Y., Tarboton, D. G. and Lin, P.: From Forecast Hydrology to Real-Time Inundation Mapping at Continental Scale, in AGU Fall Meeting, Available from: https://agu.confex.com/agu/fm16/meetingapp.cgi/Paper/186012, 2016.

410

415

Tables and Figures

Table 1: USGS study sites used in this study. For each study site the location, ID, river(s), USGS streamgage, model length, and reference are provided.

Location	ID	River(s)	USGS Streamgage Number	Model Length (km)	Reference
Spencer, IN	IN	White River	03357000	8.5	Nystrom (2013)
Fort Morgan, CO	CO	S. Platte River	06759500	7.2	Kohn and Patton (2018)
Greenville, SC	SC	Saluda	02162500	6.4	Benedict et al. (2013)
Pee Dee, NC	NC	Pee Dee River	02126375	17.0	Smith and Wagner (2016)
Hattiesburg, MS	MS	Leaf and Bouie Rivers	02473000	10.9	Storm (2014)
Charlemont, MA	MC	Deerfield River	01168500	14.6	Lombard and Bent (2015)
West Deerfield, MA	MW	Deerfield River	01170000	14.3	Lombard and Bent (2015)

420

425

430

435

440

Table 2: Base flow and Low, Medium (Med), and High flow rates for each study site.

ID	Base Flow (m³ s⁻¹)	Low Flow (m³ s⁻¹)	Med Flow (m³ s⁻¹)	High Flow (m³ s⁻¹)
IN	83.9	164.0	577.7	2027.5
CO	16.6	79.9	577.7	2814.7
SC	17.2	79.6	222.9	373.8
NC	145.4	911.8	3021.1	7391.8
MS	63.5	999.6	1730.2	3409.3
MC	25.9	311.5	996.8	2415.4
MW	38.2	455.9	1659.4	3344.2

445

450

455

460

465

Table 3: F-statistic (*F*, percentage) and error bias (*E*) for each flow scenario at all seven test locations. *F* ranges between 0 and 100% with a value of 100% indicating perfect fit between the AutoRoute and USGS flood inundation maps. *E* values less than 1 indicate a bias towards underestimation, *E* values greater than 1 indicate a bias towards overestimation, and an *E* value of 1 indicates no bias.

Location	Flow Scenario	F (%)	E
IN	Low	78.2	8.22
	Med	63.0	2.60
	High	81.7	0.11
CO	Low	63.1	0.70
	Med	62.2	0.15
	High	83.2	0.18
SC	Low	71.6	2.59
	Med	60.6	0.39
	High	65.9	0.12
NC	Low	39.3	10.97
	Med	92.6	1.32
	High	87.7	0.15
MS	Low	46.1	3.49
	Med	67.6	0.49
	High	70.2	0.20
MC	Low	80.0	2.62
	Med	76.7	2.10
	High	80.0	2.25
MW	Low	65.0	1.02
	Med	67.5	0.09
	High	74.0	0.17

470
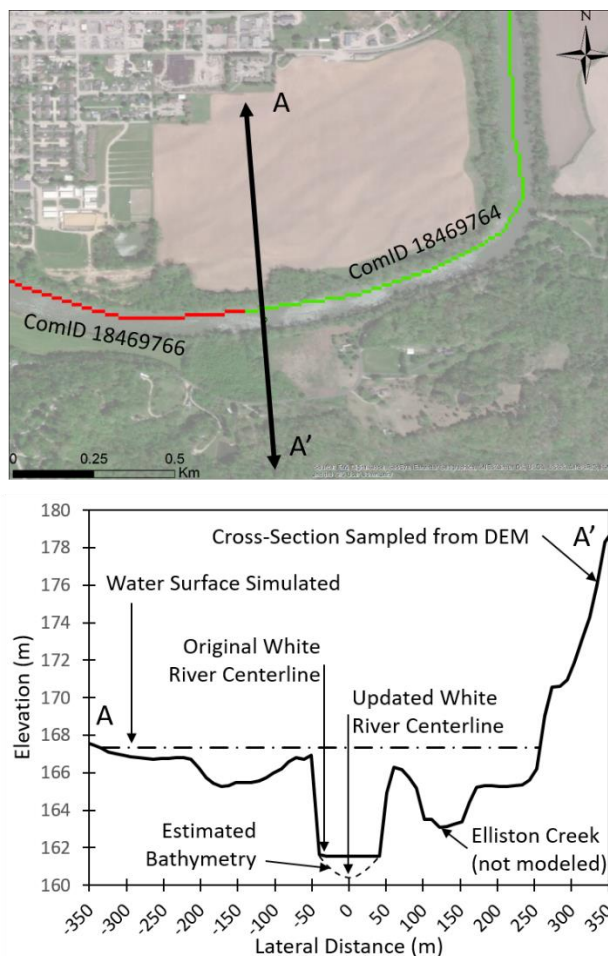
Figure 1: Cross-section profile of the White River near Spencer, IN. Sources of the background imagery in Figures 1-9 include ESRI, DigitalGlobe, Earthstar Geographics, CNES/Airbus DS, GeoEye, USDA FSA, USGS, Getmapping, Aerogrid, IGN, IGP, and the GIS User Community.
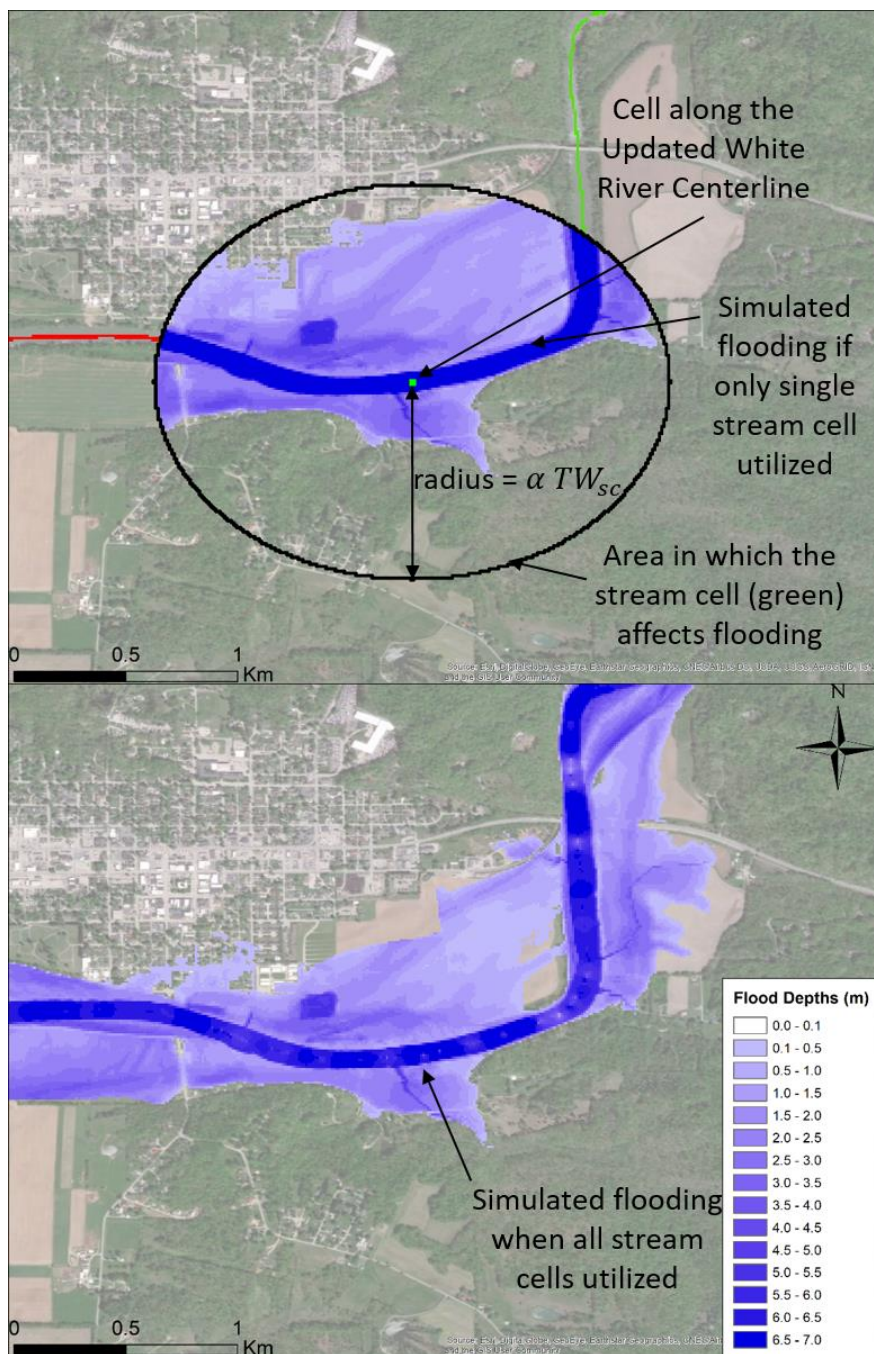
Figure 2: Top shows flood depths of surrounding terrain from at a single stream cell. Notice the area of influence (cells within radius=$\alpha\,TW_{sc}$) appears elliptical due to projection of the map. Bottom shows flood depths along the river when the depth from all stream cells are utilized. Notice that some areas shown as flooded in top figure are not flooded in bottom figure due to the influence of stream cells with lower depth calculations.

485
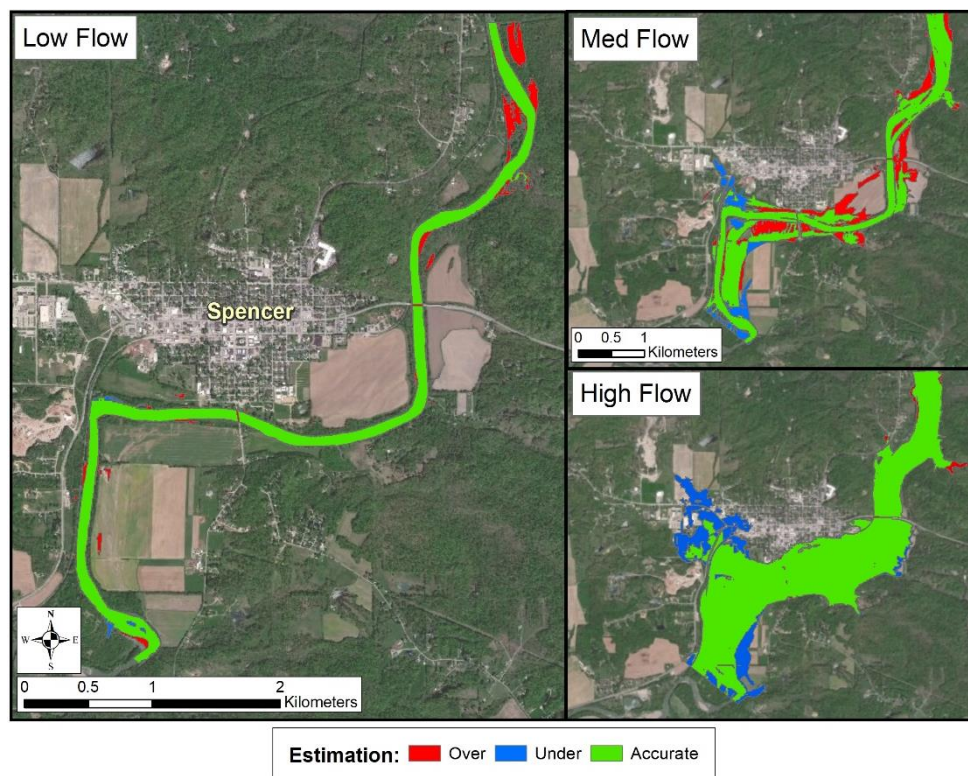
Figure 3: Spencer, IN, (IN) flood map comparison between AutoRoute simulations and USGS flood maps. Areas shaded green (Accurate) indicate areas where AutoRoute and the USGS flood maps agree. Areas shaded red (Over) indicate where only AutoRoute simulates the area as flooded. Areas shaded blue (Under) indicate where only the USGS shows the area as flooded.

490
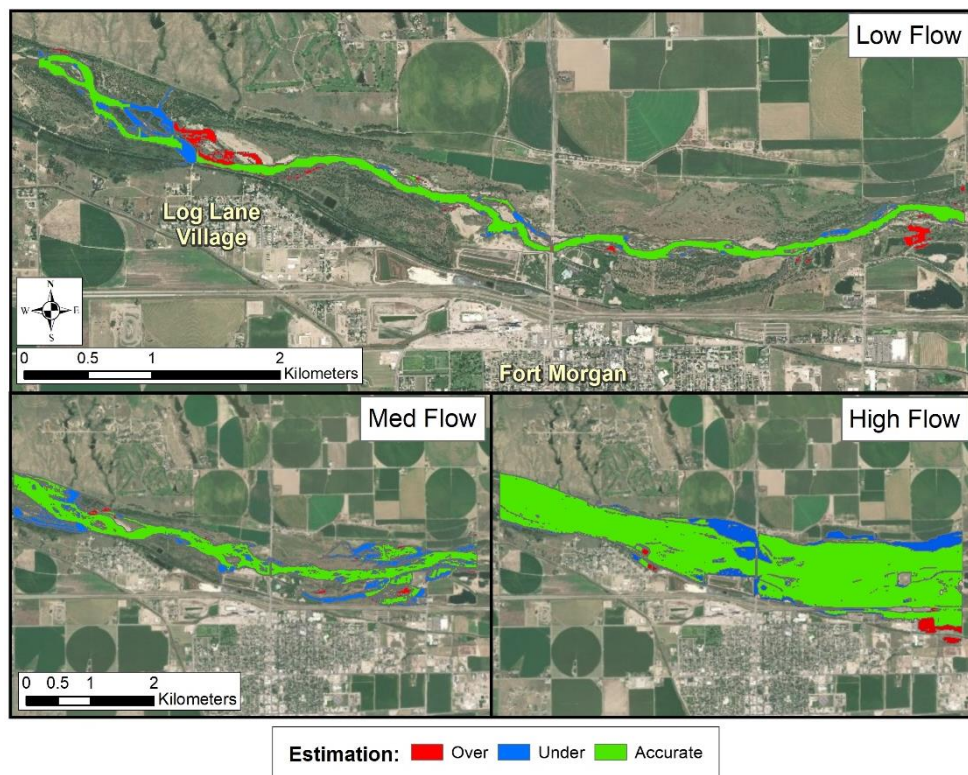
Figure 4: Fort Morgan, CO (CO) flood map comparison between AutoRoute simulations and USGS flood maps. Areas shaded green (Accurate) indicate areas where AutoRoute and the USGS flood maps agree. Areas shaded red (Over) indicate where only AutoRoute simulates the area as flooded. Areas shaded blue (Under) indicate where only the USGS shows the area as flooded.

495
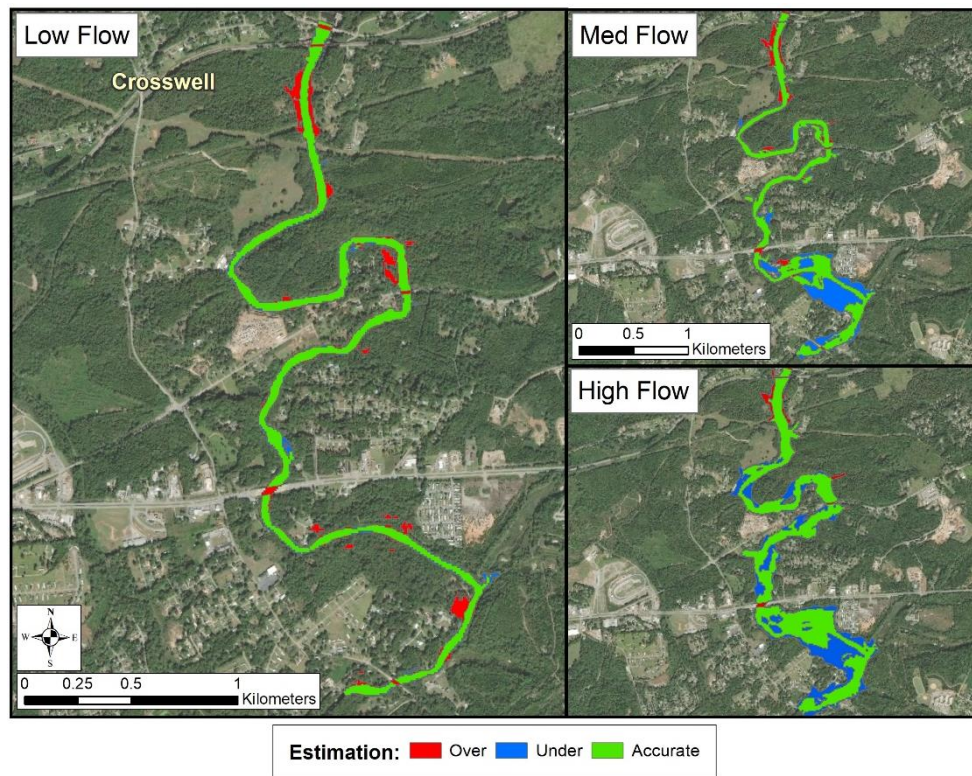
Figure 5: **Greenville, SC (SC) flood map comparison between AutoRoute simulations and USGS flood maps. Areas shaded green (Accurate) indicate areas where AutoRoute and the USGS flood maps agree. Areas shaded red (Over) indicate where only AutoRoute simulates the area as flooded. Areas shaded blue (Under) indicate where only the USGS shows the area as flooded.**

500
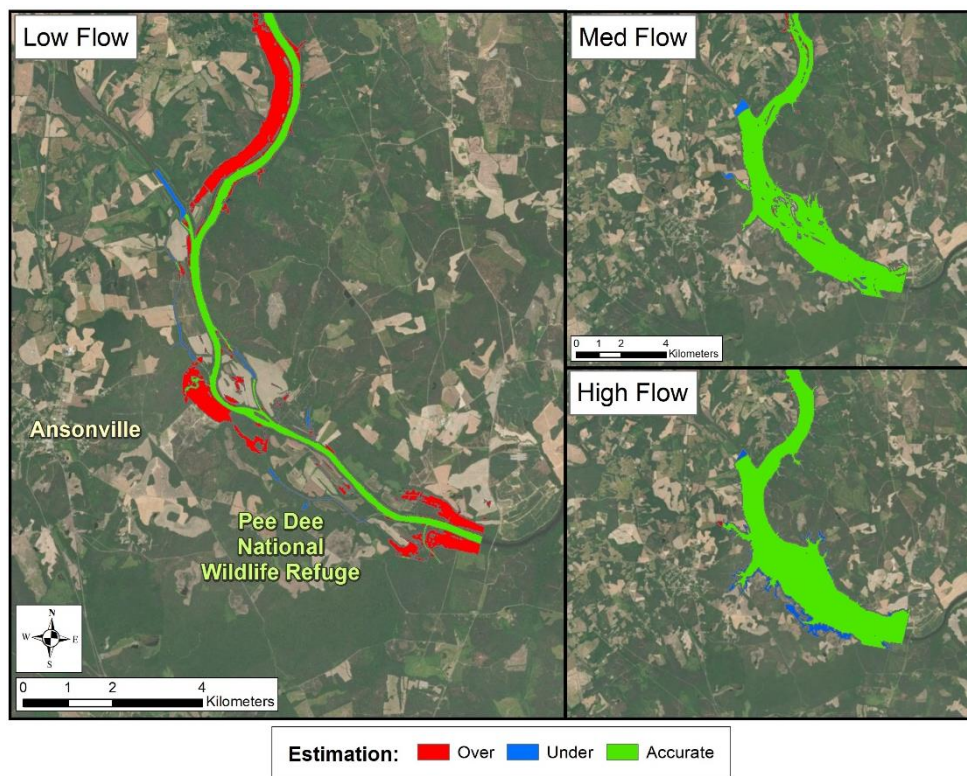
Figure 6: Pee Dee, NC (NC) flood map comparison between AutoRoute simulations and USGS flood maps. Areas shaded green (Accurate) indicate areas where AutoRoute and the USGS flood maps agree. Areas shaded red (Over) indicate where only AutoRoute simulates the area as flooded. Areas shaded blue (Under) indicate where only the USGS shows the area as flooded.

505
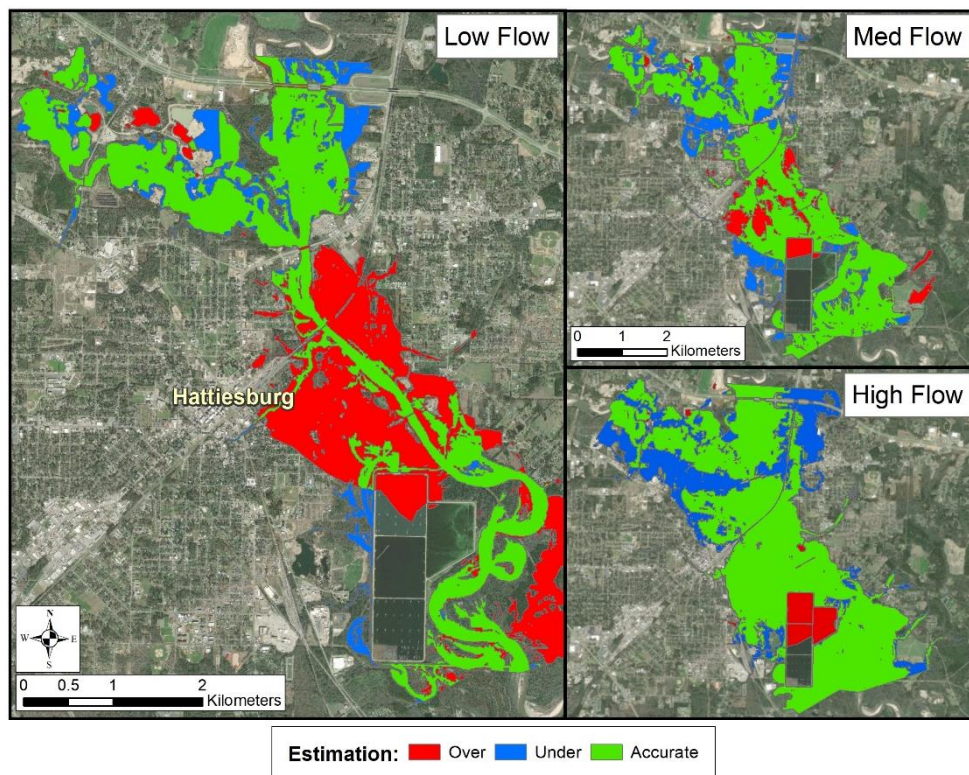
Figure 7: Hattiesburg, MS (MS) flood map comparison between AutoRoute simulations and USGS flood maps. Areas shaded green (Accurate) indicate areas where AutoRoute and the USGS flood maps agree. Areas shaded red (Over) indicate where only AutoRoute simulates the area as flooded. Areas shaded blue (Under) indicate where only the USGS shows the area as flooded. Some of the overestimation in the model simulation occurs water treatment ponds, which were not included in the USGS flood maps and can bias the results.

510
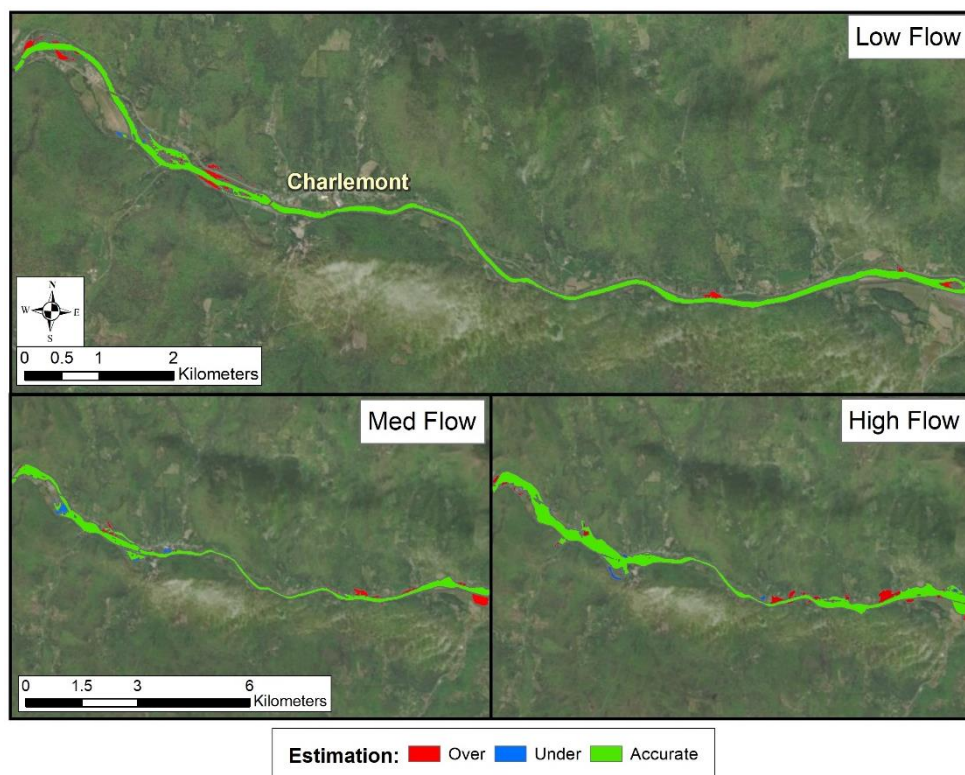
Figure 8: Charlemont, MA (MC) flood map comparison between AutoRoute simulations and USGS flood maps. Areas shaded green (Accurate) indicate areas where AutoRoute and the USGS flood maps agree. Areas shaded red (Over) indicate where only AutoRoute simulates the area as flooded. Areas shaded blue (Under) indicate where only the USGS shows the area as flooded.
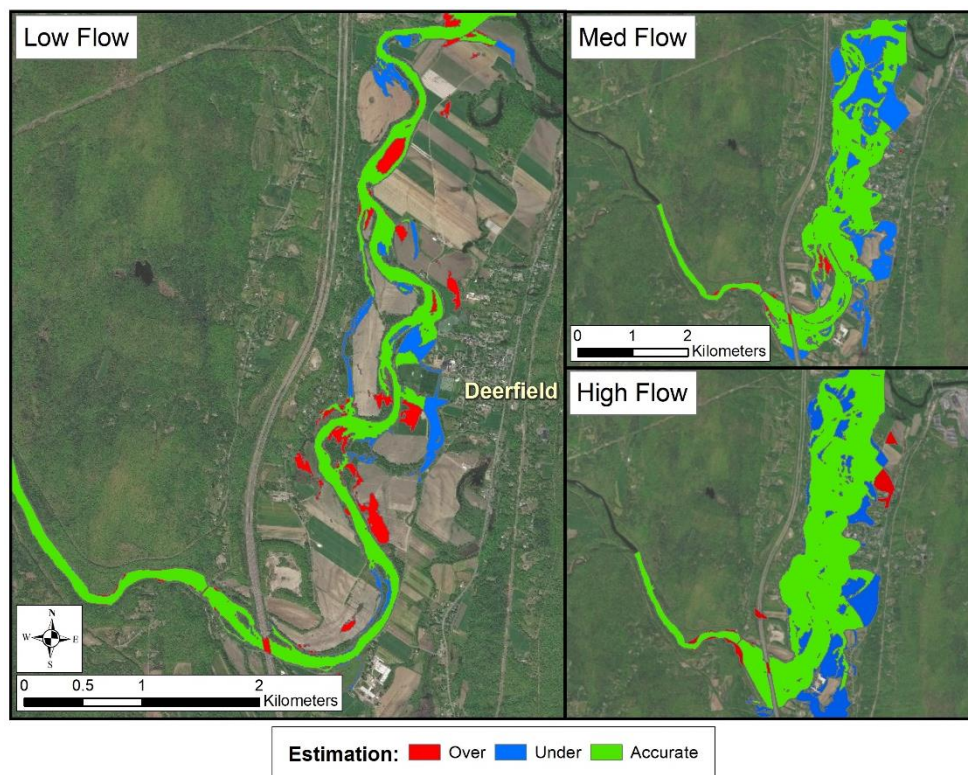
Figure 9: West Deerfield, MA (MW) flood map comparison between AutoRoute simulations and USGS flood maps. Areas shaded green (Accurate) indicate areas where AutoRoute and the USGS flood maps agree. Areas shaded red (Over) indicate where only AutoRoute simulates the area as flooded. Areas shaded blue (Under) indicate where only the USGS shows the area as flooded.